APL Materials

Photophysics of lead-free tin halide perovskite films and solar cells

Cite as: APL Mater. **7**, 080903 (2019); https://doi.org/10.1063/1.5109704
Submitted: 11 May 2019 . Accepted: 29 July 2019 . Published Online: 15 August 2019

Taketo Handa, Atsushi Wakamiya, and Yoshihiko Kanemitsu

Photophysics of lead-free tin halide perovskite films and solar cells

Cite as: APL Mater. 7, 080903 (2019); doi: 10.1063/1.5109704
Submitted: 11 May 2019 • Accepted: 29 July 2019 •
Published Online: 15 August 2019

Taketo Handa, Atsushi Wakamiya, and Yoshihiko Kanemitsu[a]

AFFILIATIONS

Institute for Chemical Research, Kyoto University, Uji, Kyoto 611-0011, Japan

[a]Author to whom correspondence should be addressed: kanemitu@scl.kyoto-u.ac.jp

ABSTRACT

The last five years have seen very active research in the field of environmentally friendly lead-free perovskite solar cells. Tin halide perovskites are certainly one of the most promising alternatives to lead-based perovskites, while the performance of present tin-based perovskite solar cells is still relatively low. Nevertheless, recent experiments on thin films with improved quality have indicated that tin halide perovskites can, in principle, provide a high device performance. In this Perspective, we summarize recent progress in the understanding of the fundamental photophysics of tin halide perovskite thin films. To identify the reason for the low performance of present devices, we discuss the energy loss mechanisms in solar cell structures from the viewpoint of photocarrier dynamics.

I. INTRODUCTION

Metal halide perovskites are semiconductor materials that have been subject to investigations for a long time, and consequently, much knowledge regarding their physical and chemical properties has been accumulated. In the early stages of research, their phase transitions and structural properties were in the focus of investigations.[1,2] In the 1990s, layered organic–inorganic hybrid perovskites received much attention and exciton photophysics at low temperatures were studied.[3–5] In the year 2009, the first solar cell based on lead halide perovskite was reported.[6] Then, after the report of the all-solid-state perovskite solar cell in 2012,[7,8] halide perovskite solar cells started to become a very active research field all over the world. Presently, solar cells based on lead halide perovskites exhibit high power conversion efficiencies and are rapidly approaching the commercialization stage. At the same time, these perovskites themselves show unique luminescence properties.[9,10] For example, even when lead halide perovskites are fabricated by simple and inexpensive low-temperature solution processes, they exhibit extremely high photoluminescence (PL) quantum efficiencies at room temperature.[11–16] A photon recycling of both free-carrier and exciton luminescence has been observed in various halide perovskites because of their high PL quantum efficiencies.[15,17–21] The high PL quantum efficiency is also considered to enable new optical functionality of perovskites as light-emitting[22–24] and laser-cooling devices.[25,26] Furthermore, the recent demonstrations of efficient high-order harmonic generation and light modulation in lead halide perovskites[27,28] also suggest their utility for nonlinear optics applications.

Lead halide perovskites exhibit exceptional optoelectronic properties, but from the viewpoint of environmental issues, their lead content is considered problematic. To address the toxicity issue, the research on lead-free perovskite materials has become more active. Lead-free materials such as tin (Sn) halide perovskites,[29–32] bismuth halides,[33–35] germanium perovskites,[36] and copper halide[37] have been reported. In particular, the tin halide perovskites are attracting much attention because they have achieved relatively high solar cell efficiencies; 9.6% has been reported for tin iodide perovskite.[38] However, this is still significantly lower than the conversion efficiencies of over 23% realized for lead halide perovskite solar cells.[39–42] It is important to clarify whether the presently realized efficiencies are limited by the fabrication technology or the intrinsic material properties. Thus, large efforts have been devoted to the improvements of the film preparation method and also the device structure. On the other hand, until recently, the understanding of the optical properties of tin perovskites had not advanced much. Owing to recent improvements in the thin film quality, it has become possible to clarify the intrinsic optical properties of tin halide perovskites. The knowledge of these fundamental optical properties

of the semiconductor layer is essential since they determine the upper limit of the device performance and the optimum device structure.[9,10]

In this Perspective, we provide a summary of the recent progress in the research of the fundamental optical properties of tin halide perovskites. By comparing the physical properties of tin- and lead-based perovskites, we discuss similar features as well as differences between them. We also discuss the origin and possible solutions of the low performances of present lead-free tin perovskite solar cells from the viewpoint of carrier dynamics.

II. BANDGAP ENGINEERING AND FILM QUALITY IMPROVEMENT

Before we go into the detailed discussion of the optical properties, an overview of the structural properties of the perovskite material class is provided. The chemical formula of metal halide perovskites can be written as ABX_3 [Fig. 1(a)]. The A site contains an organic material [e.g., CH_3NH_3 (also called MA) or $CH(NH_2)_2$ (also called FA)] or an inorganic element (Cs) as a monovalent cation. The B site contains a divalent metal ion (e.g., Pb or Sn), and the X site is occupied by a halogen (Cl, Br, or I). The stability of the ABX_3 structure is determined by the tolerance factor and the octahedral factor, which are calculated from the ionic radii of the elements or molecules at A, B, and X sites.[43–45] These sites can be occupied uniformly by a single element or molecule, or some combination of ionic species can be substituted into the lattice. The use of such mixed-cation or mixed-halide perovskites significantly improves the stability of device performance.[46–48] By controlling the composition, their luminescence color can be tuned continuously over a wide wavelength range from the near-infrared to the blue.[49–52] Figure 1(b) summarizes the bandgap energies of several perovskites suited for solar cell devices and their reported conversion efficiencies.

The bandgap energy (E_g) of a semiconductor is important when considering the application in solar cell devices since it determines the theoretical upper limit of the solar cell efficiency via the detailed balance principle.[53] In order to achieve an efficient device, it is important to bear in mind that the optimum E_g depends on the number of junctions and on the PL quantum efficiency of the used material.[54] For example, if the PL quantum efficiency becomes smaller than unity, the optimum E_g for the highest possible solar cell efficiency becomes larger.[55] The PL quantum efficiency depends on the recombination dynamics of photocarriers in the material and is discussed in Sec. IV.

The narrowest bandgap of the lead-based perovskites is that of $FAPbI_3$, 1.48 eV.[56] In case of a PL quantum efficiency of 100%, the optimum bandgap energy E_g for a single-junction solar cell is 1.34 eV under AM 1.5G solar illumination as derived from the detailed balance theory. This E_g cannot be obtained by lead-based perovskites. In this respect, tin halide perovskites are more suited because they can reach narrower E_g than the lead perovskite counterparts.[29–32] Furthermore, it has been reported that the E_g of the Pb–Sn mixed perovskite $APb_{1-x}Sn_xI_3$ changes in a characteristic nonlinear manner with respect to the Sn content x.[57–60] Figure 1(c) summarizes the reported E_g values of $APb_{1-x}Sn_xI_3$ estimated from absorption spectra in the literature.[57–60] It can be confirmed that E_g reaches a minimum in the x range from about 0.5–0.75, and this trend is preserved even when different A-site cations are employed. As possible origins of this nonlinear change of the bandgap, the competition between spin–orbit interaction and the lattice distortion effect,[61] the short-range order of the Pb–Sn configuration,[59] and the atomic orbital mismatch between Pb and Sn[62] have been suggested. While the similar trend can be seen among the different reports in Fig. 1(c), the absolute values of E_g vary even for the same composition. The quality of the used thin film and the employed measurement methods can be considered as possible origins of the large difference in the reported values.[63] Furthermore, in the tin halide perovskites, the onset of photoabsorption is very sensitive to the amount of doping.[64] This issue is discussed in detail in Sec. III. In any case, the use of Sn results in a large bandgap tunability, and this is advantageous for the design of solar cell devices including multijunction cells.

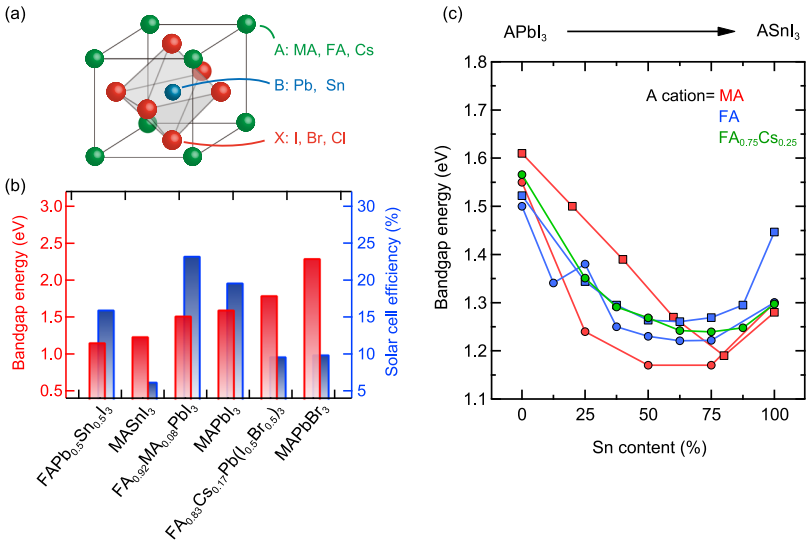

FIG. 1. (a) Crystal structure of ABX_3 halide perovskites. (b) Reported bandgap energies and solar cell efficiencies of several halide perovskites. Data are taken from Refs. 15, 30, 42, 51, 59, 64, 65, 151, and 170. (c) Nonlinear bandgap shift of $APb_{1-x}Sn_xI_3$ as a function of the Sn content. Data are taken from Refs. 57–60.

Although tin halide perovskites are important in terms of their potential as lead-free materials and from the viewpoint of bandgap tunability, the present efficiencies of the lead-free tin-based perovskite solar cells are not as high as those of lead-based perovskite solar cells [Fig. 1(b)]. To understand what is needed to realize more efficient solar cells based on tin halide perovskites, we briefly summarize the optical properties of lead halide perovskites. Owing to the extremely large number of publications in the last decade, many exceptional properties of lead halide perovskites have been revealed, i.e., a large absorption coefficient in the visible region originating from direct band transitions,[65–68] a sharp absorption edge with a low number of localized states within the bandgap,[69,70] PL with almost no Stokes shift,[71,72] a high PL quantum efficiency,[11–16] an efficient electron–phonon interaction,[73–76] anti-Stokes luminescence,[25,26,77,78] photon recycling,[15,17–21,79] a small exciton binding energy,[71,80,81] and extremely long lifetimes and long diffusion lengths of photocarriers.[11,17,18,82–84]

On the other hand, the understanding of the fundamental optical properties of tin halide perovskites had not progressed until very recently. The fabrication of high-quality samples is essential to understand intrinsic optical properties of a semiconductor material. However, the tin halide perovskites used in the early stages of research were strongly influenced by extrinsic factors, such as impurities, defects, and traps, preventing in-depth discussions of their intrinsic optical properties.[85,86] Fortunately, recent improvements in film deposition techniques made the detailed discussions possible.

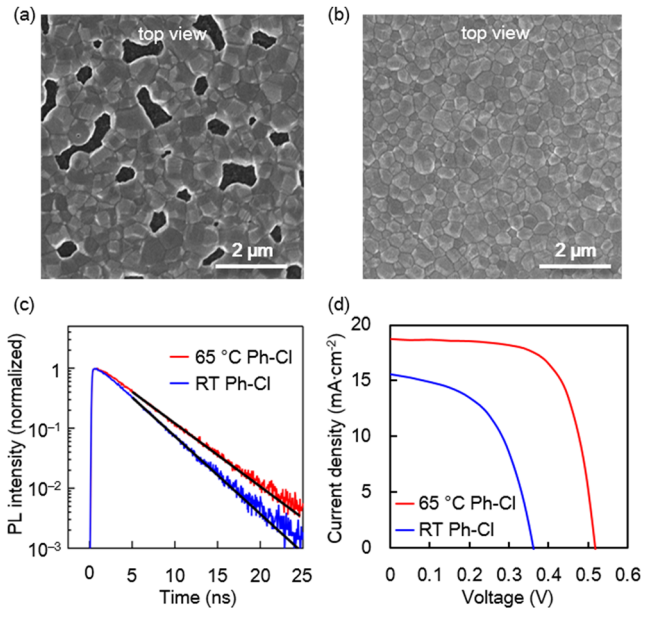

FIG. 2. Scanning electron microscope images of $FA_{0.75}MA_{0.25}SnI_3$ films fabricated with (a) room-temperature (RT) chlorobenzene (Ph-Cl) and (b) preheated chlorobenzene at 65 °C. (c) PL decay curves of $FA_{0.75}MA_{0.25}SnI_3$ films and (d) I–V curves under 1-sun illumination of $FA_{0.75}MA_{0.25}SnI_3$ solar cells prepared with room-temperature (blue line) or 65 °C preheated chlorobenzene (red line) as antisolvent. Adapted with permission from Liu *et al.*, Angew. Chem., Int. Ed. **57**, 13221 (2018). Copyright 2018 Wiley-VCH.

In the following, some details regarding the progress in preparation techniques are provided.

At first, it should be noted that the crystallization of tin-based perovskites is fast, and thus, the control of the crystal growth is difficult.[30,87–90] Without careful preparation procedure, high-quality samples cannot be obtained. The reproducibility of the device performance was also reported to be low at the early stage of the research.[30] Recent studies have clarified that a better film quality can be obtained via slower crystallization by utilizing an appropriate solvent[31,87] and employing an antisolvent during the spin-coating process.[91–93] By using these methods, thin films with better crystalline quality and improved coverage of the substrate can be achieved, which consequently leads to a better performance and reproducibility of solar cell devices. Recently, Ozaki *et al.*[94] reported the importance of the purity of the precursor, and they have developed highly-purified materials using tin halide complexes. Furthermore, as a simple but effective film deposition method, Liu *et al.*[95] have developed a hot antisolvent treatment (HAT). Instead of the room-temperature antisolvent, they dropped a 65-°C pre-heated antisolvent on the precursor solution during spin coating and succeeded in obtaining a perovskite film with improved coverage [see Figs. 2(a) and 2(b)].[95] In the tin perovskite thin films prepared by the HAT method, an increase in the photocarrier lifetime was observed, which suggests suppression of nonradiative recombination centers [Fig. 2(c)]. Accordingly, by employing this HAT method, the device performance and reproducibility were improved [Fig. 2(d)]. These improvements in the fabrication of tin halide perovskite thin films have contributed to the recent progress in the understanding of the fundamental optical properties of tin halide perovskites.

III. OPTICAL ABSORPTION AND PHOTOLUMINESCENCE

A. Luminescence Stokes shift

In this section, the steady-state optical spectra near the band edge are elaborated. Figures 3(a) and 3(b) present the PL and absorption spectra of $MASnI_3$[64] and $FA_{0.75}MA_{0.25}SnI_3$,[95] respectively. These thin films were prepared by adding SnF_2 to the precursor solution. The role of SnF_2 during the film fabrication is discussed in Sec. III B. For both $MASnI_3$ and $FA_{0.75}MA_{0.25}SnI_3$, a sharp onset of the absorption is observed. This indicates a low number of defects within the bandgap. Less defect states imply less nonradiative recombination via processes like Shockley-Read-Hall recombination. Furthermore, it is noteworthy that almost no Stokes shift is observed between the PL peak and the absorption onset, neither for $MASnI_3$ (single A-site cation) nor for $FA_{0.75}MA_{0.25}SnI_3$ (mixed cation). The PL peak position is the effective upper limit of the open-circuit voltage (V_{oc}). The observation of a small Stokes shift and a steep absorption edge indicates small voltage losses within the bulk material.[69,96] This is important not only for solar cells, but also for light-emitting diode (LED) operation. The E_g of $MASnI_3$ is 1.26 eV, while that of $FA_{0.75}MA_{0.25}SnI_3$ is 1.36 eV. The E_g of the latter material is close to the optimum E_g for a single-junction solar cell, which shows the importance of the development of the tin halide perovskites with mixed A-site cations and their small Stokes shifts. Here, note that the optimum E_g for which the highest conversion efficiency can be expected, depends on the PL quantum efficiency of the semiconductor material.[53–55]

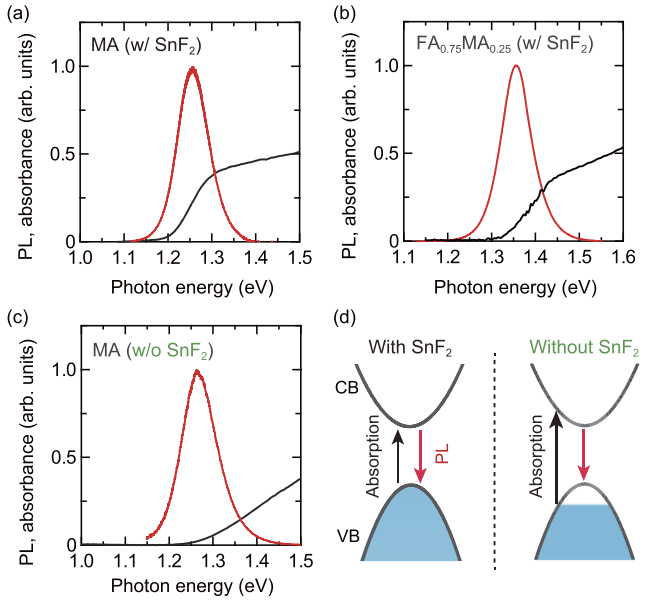

FIG. 3. PL (red line) and absorption (black line) spectra of (a) a $MASnI_3$ thin film prepared with 20 mol. % SnF_2, (b) a $FA_{0.75}MA_{0.25}SnI_3$ film prepared with 10 mol. % SnF_2, and (c) a $MASnI_3$ film prepared without using SnF_2. (d) Schematic illustration of the Burstein-Moss shift. The data in (a) and (c) are taken from Ref. 64.

B. Spontaneous hole doping and band-filling effect

In tin halide perovskites, hole doping and band-filling effects play crucial roles for the optoelectronic responses and, consequently, also for the device performance. Figures 3(a) and 3(c) show the PL and absorption spectra of the $MASnI_3$ thin films prepared with and without the SnF_2 additive, respectively.[64] It has been reported that, in tin halide perovskites, spontaneous hole doping easily occurs,[97,98] and that the addition of SnF_2 effectively reduces the hole density in the films mainly due to the suppression of the formation of tin vacancies and/or oxidation of Sn^{2+} to Sn^{4+}.[31,92,99–101] It is found that the absorption onset of the thin film prepared without SnF_2 [Fig. 3(c)] lies at a higher energy than that of the sample prepared with SnF_2 [Fig. 3(a)]. Additionally, the sample without SnF_2 shows a less steep absorption spectrum near the onset. On the other hand, the PL peak energies of the $MASnI_3$ films with and without SnF_2 are located at 1.26 and 1.27 eV, i.e., the PL peak energy hardly changes with the hole density. These experimental results can be explained by the Burstein–Moss effect (band filling effect) due to the high carrier concentration [see Fig. 3(d)].[64,102–105] In the sample without SnF_2, the states near the top of the valence band is occupied by holes. Therefore, light absorption occurs for photon energies slightly larger than the fundamental bandgap energy. In contrast, PL is emitted by the recombination between the photogenerated electrons that have relaxed to the bottom of the conduction band and the holes from the unintentional background doping. Thus, the PL peak positions of both samples are almost the same. The more gradual absorption onset is caused by increased structural disorder in the sample without SnF_2 due to the large number of Sn vacancies.

A further interesting example of exploiting the large background doping concentration in tin-based perovskites is the following: by intentionally replacing some Pb atoms by Sn inside a lead-based perovskite, it becomes possible to control the charging inside a perovskite nanoparticle layer and to increase the LED efficiency.[106] The consideration of doping and ionization is particularly important for the application of halide perovskites due to their ionic nature.[107–112] Most parts of the above discussion of the doping are about p-type tin halide perovskites. By using a different crystal growth technique, the fabrication of n-type tin iodide perovskites with high electron mobilities has been reported as well.[113] In comparison, the doping of lead perovskites is relatively difficult,[114] which can be considered as the other aspect of the usually advantageous defect tolerance of this material.[115] The doping effect is one of the most important topics for tin halide perovskites and also influences the physical properties discussed hereafter.

C. Electron–phonon interaction in tin halide perovskites

In halide perovskite crystals with the polar nature, the electron–phonon interaction plays a critical role for their optical and charge transport properties.[116] Thus, intensive studies have been performed to clarify the electron–phonon interaction,[73–76] and its possible relation to the optical properties in lead halide perovskites have been discussed.[117–133] Recently, it has become possible to obtain tin halide perovskite films with better quality owing to improved fabrication techniques, e.g., the use of SnF_2 additives[31,92] or the HAT method.[95] Therefore, the width of the PL spectrum can now be used to discuss the intrinsic physical properties. Below, the results of recent investigations on the electron–phonon interactions in tin perovskite $MASnI_3$ are provided.[134]

Figures 4(a) and 4(b) show the PL spectra of a $MASnI_3$ thin film for different temperatures and the corresponding PL full width at half-maximum (FWHM) values. The narrow PL FWHM (85 meV at room temperature) verifies that a high-quality sample is obtained by employing a mixed solution of dimethyl sulfoxide /N,N-dimethylformamide as solvent and chlorobenzene as an anti-solvent.[134] As the temperature decreases, the PL peak energy shows

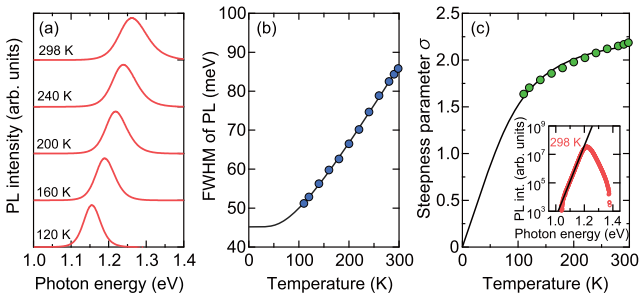

FIG. 4. (a) PL spectrum and (b) its FWHM of a $MASnI_3$ thin film at different temperatures. The black solid line in (b) is the fitting result considering the electron–LO phonon coupling. (c) Temperature dependence of the steepness parameter, which is extracted from the low-energy tail of the PL as shown in the inset. The black solid line is the theoretical prediction considering the contribution of a phonon with an energy of 22 meV. Adapted with permission from Handa *et al.*, Phys. Rev. Mater. **2**, 075402 (2018). Copyright 2018 American Physical Society.

a redshift. This tendency is opposite to that of typical inorganic semiconductors such as GaAs and Si.[116] A similar tendency has also been observed for lead halide perovskites,[65,73–76,135–137] lead chalcogenides,[138] and CuCl.[139] In the lead halide perovskites, the electron–phonon interaction,[75,139] and the temperature-induced change in the overlap between the p orbital of iodine (I) and the s orbital of Pb (which form the valence band in $APbI_3$ perovskites),[140] have been considered as possible origins of this tendency. In the temperature region below 120 K, $MASnI_3$ exhibits a complex PL response whose details are discussed in Ref. 134.

The temperature dependence of the PL FWHM can be described by the intrinsic electron–longitudinal-optical (LO) phonon coupling.[73,74,141] By fitting the temperature-dependent FWHM values using a model considering the electron–LO phonon coupling [black solid line in Fig. 4(b)], $\hbar\omega_{LO}$ = 21.6 meV and Γ_{LO} = 54 meV are obtained for the LO phonon energy and the coupling constant in $MASnI_3$, respectively.[134] From the low-energy tail of the PL spectrum, the steepness parameter σ (defined by $E_U = kT/\sigma$, where E_U is the Urbach energy) can be estimated.[142,143] It is clarified that the temperature dependence of σ can be well explained by the contribution from the above-mentioned phonon with an energy of 22 meV [black solid line in Fig. 4(c)].[134] Furthermore, the same phonon energy has also been obtained from different samples fabricated using a different method.[134] Such a confirmation of reproducibility is important when characterizing intrinsic physical properties of tin perovskites. The temperature dependence of σ in Fig. 4(c) supports that the Urbach tail of the $MASnI_3$ thin film is the intrinsic tail determined by the intrinsic electron–phonon interaction, but is not due to static impurity levels or other extrinsic factors. Actually, from σ(300 K) = 2.19, the Urbach energy of $MASnI_3$ at 300 K is calculated as E_U = 12 meV.[134] This is a remarkably small value that is comparable to the E_U of the lead perovskite $MAPbI_3$, where the small E_U is considered as one reason for the observed high V_{oc} of the $MAPbI_3$ solar cells.[69,70]

As shown above, even in the tin halide perovskites, the broadening of the optical transitions is governed by the intrinsic electron–optical phonon interactions if films with good quality are investigated.[134] This feature is very similar to that observed in lead halide perovskites.[73–76] Note, however, that the values of their LO phonon energies are different; recently, the LO phonon energies of the lead halide perovskites $MAPbX_3$ (X = Cl, Br, I) have been directly determined by using THz spectroscopy.[76] The reported value for $MAPbI_3$ is $\hbar\omega_{LO}$ = 16 meV. From this reported value for $MAPbI_3$ and the results for $MASnI_3$ in Fig. 4, we find that the optical phonon frequency shifts toward higher energies upon replacing Pb by Sn. In qualitative terms, this can be understood as the effect of inserting the lighter Sn atom.

It is known that in the lead halide perovskites, the effective electron–LO phonon coupling leads to an intrinsic broadening.[77,78] In order to explore this feature, the results of resonant PL measurements on $MASnI_3$[64] and $MAPbI_3$[78] are shown in Figs. 5(a) and 5(b), respectively. In both samples, the shape of the PL spectra does not depend on the excitation energy. This is consistent with the absence of a notable Stokes shift of the PL (Fig. 3) and also the temperature dependence of the PL FWHM (Fig. 4). Furthermore, even when the excitation energy is below the PL peak energy, a strong anti-Stokes luminescence signal appears. The observation of anti-Stokes luminescence suggests an upconversion

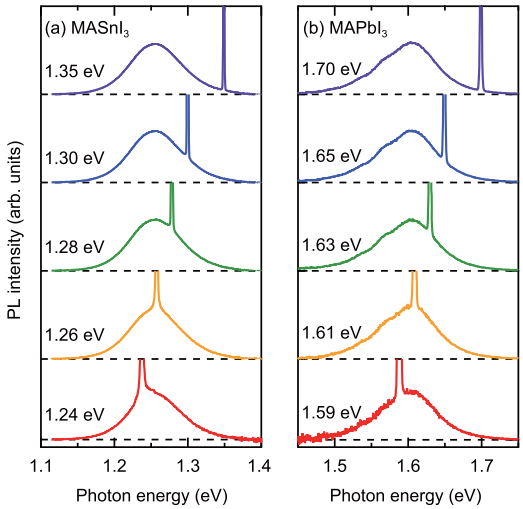

FIG. 5. PL spectra under resonant excitation of (a) a $MASnI_3$ thin film prepared with 20 mol. % SnF_2 and (b) a $MAPbI_3$ thin film. The excitation photon energies are shown in the figure. The diverging peaks in the spectra originate from the scattering of the excitation light.

mechanism inside the material, presumably by the assistance of phonons. Importantly, in the lead halide perovskites, the strong anti-Stokes luminescence coupled with a high luminescence quantum efficiency[12–16] can be implemented to achieve efficient laser cooling.[25,26] In Ref. 26, one can find detailed discussions on laser cooling, including the relation between laser cooling and photon recycling and the observation of anti-Stokes luminescence in optically thick samples.

D. Charge carrier mobility and exciton binding energy

The effective mass of charge carriers is an important physical parameter for transport properties and many other physical properties. First-principle calculations have shown that the tin iodide perovskite possess a more dispersive band and smaller effective mass than its lead perovskite counterparts.[66] The smaller effective masses indicate higher carrier mobilities in tin halide perovskites; actually, carrier mobilities on the order of 100 $cm^2/(V\ s)$ have been reported in thin films and polycrystalline samples of tin iodide perovskites ($MASnI_3$, $FASnI_3$, and $CsSnI_3$).[98,100,113,144] These values are larger than the reported mobilities of lead halide perovskites, which possess carrier mobilities in the range from a few to few tens of $cm^2/(V\ s)$.[84,113,145–148]

The exciton binding energy is also important when considering the recombination kinetics of photogenerated carriers and their transport processes. Recently, by low-temperature magnetospectroscopy, the exciton binding energy in the Sn-dominant $MASn_{0.8}Pb_{0.2}I_3$ has been measured to be 16 meV.[149] This is almost the same as that of $MAPbI_3$,[80,81] in which the room-temperature optical responses are governed by free-carriers.[11] Thus, similar free-carrier like photoresponses are expected for tin iodide perovskites, and this can be confirmed by the absorption spectra with no excitonic peak (see Fig. 3).

As described above, the optical spectra obtained from $MASnI_3$ and $MAPbI_3$ thin films under steady-state excitation conditions are very similar. Therefore, both seem to be suited for various optoelectronic applications. However, as mentioned at the beginning of this Perspective, the conversion efficiencies of tin- and lead-based perovskite solar cells differ strongly. This indicates that dynamic properties of photocarriers including carrier lifetimes, diffusion, and other recombination kinetics are strongly different. In fact, the dynamic behaviors of photocarriers govern the photovoltaic properties as shown below.

IV. PHOTOCARRIER DYNAMICS AND ENERGY LOSS PROCESSES

A. Energy losses in solar cells

First, the energy losses in a tin perovskite solar cell are briefly analyzed through the PL and absorption spectra for a thin-film sample and the current–voltage (I–V) curve of a solar cell device (Fig. 6). This plot intuitively explains the energy loss processes.[10,150] The I–V curve in Fig. 6(a) is obtained for a regular-structure solar cell comprising a glass/fluorine-doped tin oxide (FTO)/compact TiO_2/mesoporous TiO_2/$MASnI_3$/poly(triaryl amine) (PTAA)/Au structure.[64] Due to the narrow bandgap of $MASnI_3$ and a thick absorber layer of about 500 nm, a relatively high short-circuit current density (J_{sc}) of 26.1 mA/cm^2 is obtained. While this value exceeds the current density obtained in lead-based perovskite solar cells, it is only 67% of the upper limit that can be determined by the E_g of $MASnI_3$, indicating a large current loss. Note that, in a $MAPbI_3$ solar cell, a J_{sc} of 91% of the theoretical upper limit has been obtained,[151] and also in other types of semiconductor solar cells, the current loss is usually small.[152] The figure also shows the presence of large losses in V_{oc} and the fill factor (FF).

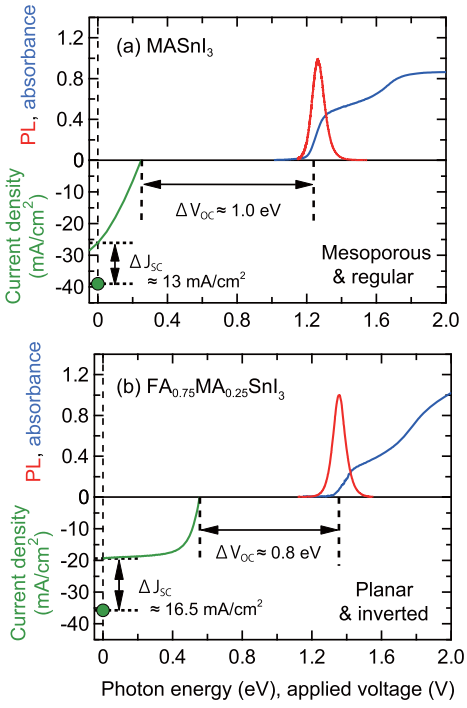

FIG. 6. Optical and electrical characterization of (a) a regular-type $MASnI_3$ solar cell (prepared with 20 mol. % SnF_2) and (b) an inverted-type $FA_{0.75}MA_{0.25}SnI_3$ solar cell (prepared with 10 mol. % SnF_2). The optical absorption (blue lines) and PL spectra (red lines) are shown in the upper panels, and the illuminated I–V curves are shown in green in the lower panels. The upper limit of J_{sc} calculated from the bandgap energy is shown with green filled circles. The data in (a) are taken from Ref. 64, while those in (b) taken from Ref. 95.

Recent works have shown that the voltage losses in tin-based perovskite solar cells can be suppressed by using an inverted architecture.[90,92,95,153–155] Figure 6(b) shows the I–V curve of an inverted planar-structure solar cell, comprising a glass/indium tin oxide (ITO)/poly(3,4-ethylenedioxythiophene):poly(styrenesulfonic acid) (PEDOT:PSS)/$FA_{0.75}MA_{0.25}SnI_3$/C_{60}/bathocuproine (BCP)/Ag layer structure.[95] By applying the inverted structure, the V_{oc} drop reduces and also the FF improves; a V_{oc} of 0.55 V and an efficiency of 7.2% are obtained.[95] However, the J_{sc} value still stays at only 54% of the limit expected from E_g = 1.36 eV. One advantage of tin-based perovskites is the possible high current density due to their narrow bandgap. However, the J_{sc} values achieved so far in tin-based perovskite solar cells, are well below the theoretical J_{sc} determined by E_g. In other words, the advantage of this material system has not yet been fully exploited. The improvement in J_{sc} is indispensable for the efficiency improvement of tin-based perovskite solar cells.

B. Photocarrier recombination and transport dynamics

Time-resolved PL measurements enable a detailed investigation of operating mechanism of solar cells including photocurrent loss processes.[10,156–160] Figure 7 summarizes the photocarrier density dependence of the PL lifetimes of the $FA_{0.75}MA_{0.25}SnI_3$ thin film (prepared using SnF_2), the $MAPbI_3$ thin film, and the solar cell devices based on these films.[159] In the $MAPbI_3$ thin film [Fig. 7(a); blue filled circles], the PL lifetime is long under weak excitation and becomes shorter for higher excitation fluences. This dependence can be explained by the bimolecular radiative recombination of free electrons and holes.[11] The long lifetime under weak excitation indicates the low density of nonradiative recombination centers. On the other hand, the PL lifetime of the $FA_{0.75}MA_{0.25}SnI_3$ thin film [Fig. 7(b); blue filled circles] is extremely short and shows almost no reduction even under high excitation fluences. This indicates that the PL lifetime of the $FA_{0.75}MA_{0.25}SnI_3$ film is mainly determined by nonradiative recombination via a large number of defect states, probably originating from the formation of tin vacancies and/or the oxidation of Sn^{2+}. We note that the PL lifetime of tin perovskite films is further shortened by more than one order of magnitude if SnF_2 is not added to the precursor solution.[64,161] The use of a stronger reducing agent that more effectively suppresses the vacancy formation and/or tin oxidation could lead to longer carrier lifetimes.

When the above perovskite layers are incorporated in solar cell devices, the PL lifetimes become much faster than that of the bare thin films [Figs. 7(a) and 7(b); red filled circles]. This is a result of the carrier extraction from the perovskite layer to the transport layers, which cause a faster reduction of the photocarrier density in the absorber layer.[159,162] Note that the data shown with red in Fig. 7(a) are obtained for a regular mesoporous

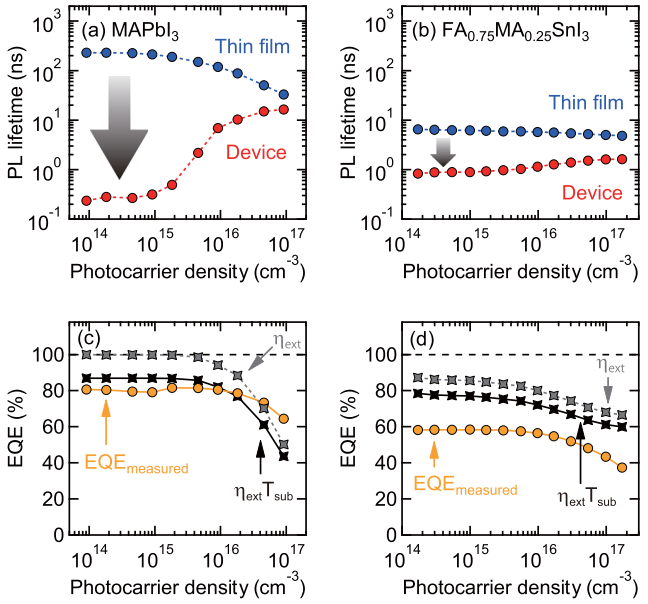

FIG. 7. Photocarrier density dependences of the PL lifetimes of the bare thin film (blue filled circles) and solar cell device (red filled circles) based on (a) $MAPbI_3$ and (b) $FA_{0.75}MA_{0.25}SnI_3$ fabricated with 10 mol. % SnF_2. The PL lifetimes here are defined as the time that the PL intensity drops to 1/e of the initial intensity. The excitation wavelengths are 650 nm and 444 nm for (a) and (b), respectively. Photocarrier density dependences of electrically measured EQE (orange filled circles) of solar cells based on (c) $MAPbI_3$ and (d) $FA_{0.75}MA_{0.25}SnI_3$ with 10 mol. % SnF_2. The grey stars show the carrier extraction efficiencies (η_{ext}) calculated from the PL lifetimes in the film and the device shown in (a) and (b). The black stars are the effective carrier extraction efficiencies considering the transmittance of the substrate ($\eta_{ext}T_{sub}$). Data in (a) and (c) are taken from Ref. 159.

structure (glass/FTO/compact TiO_2/mesoporous TiO_2/$MAPbI_3$/2,2′,7,7′-tetrakis(N,N-di-*p*-methoxyphenylamine)-9,9′-spirobifluorene (spiro-OMeTAD)/Au), while those in Fig. 7(b) are obtained for an inverted planar structure (glass/ITO/PEDOT:PSS/$FA_{0.75}MA_{0.25}SnI_3$/C_{60}/BCP/Ag). The particularly large difference between the lifetimes of the $MAPbI_3$ film and the solar cell device under weak excitation reflects a very high extraction efficiency under short-circuit conditions.[159] In the $MAPbI_3$ solar cell, a significantly prolonged PL lifetime is observed for increased excitation fluences [Fig. 7(a)].[159] This means that long-lived carriers are generated in the absorber layer and the Fermi-level shifts strongly. Such a prolonged carrier lifetime indicates a reduction of the carrier extraction efficiency at the interfaces under strong excitation conditions.

In Fig. 7(b), a similar tendency can be seen for the $FA_{0.75}MA_{0.25}SnI_3$ solar cell, but the magnitude of the increase in PL lifetime under strong excitation is not as strong as that observed in the $MAPbI_3$ solar cell. This is because the PL lifetime in the former device is dominated by the fast nonradiative bulk recombination in the tin perovskite layer.[64] These results indicate a short carrier diffusion length in the $FA_{0.75}MA_{0.25}SnI_3$ layer, which leads to a lower solar cell performance.

Furthermore, the quantitative comparison between the lifetimes of the thin film and solar cell device allows for the elucidation of the J_{sc} loss mechanisms in the device. By using the PL lifetime in the thin film sample (τ_{film}) and that in the device (τ_{device}), the carrier extraction efficiency can be calculated via $\eta_{ext} = 1 - \tau_{device}/\tau_{film}$ for low carrier densities.[159] In Figs. 7(c) and 7(d), the η_{ext} values are compared with the measured external quantum efficiencies (EQE) for the lead- and tin-based solar cells, respectively. The product of η_{ext} and the transmittance of the transparent substrate ($\eta_{ext}T_{sub}$) is also shown. In Fig. 7(c), it can be confirmed that η_{ext} of the $MAPbI_3$ solar cell is nearly unity in the weak excitation regime owing to the large difference in τ_{film} and τ_{device}, and that $\eta_{ext}T_{sub}$ almost coincides with the experimental EQE.[159] On the other hand, in the $FA_{0.75}MA_{0.25}SnI_3$ solar cell, the η_{ext} is less than unity as a result of the fast carrier lifetime in the thin film [Fig. 7(d)]. Furthermore, the observed EQE is less than $\eta_{ext}T_{sub}$ by about 20%, due to the large transmission losses of the thin perovskite layer. Overall, in the tin-based perovskite solar cells, both the small η_{ext} (due to the dominant nonradiative recombination within the absorber layer) and the large transmission loss (due to the thin absorber thickness) should be improved to obtain a better J_{sc}.

Finally, the V_{oc} losses are discussed. Even in the tin perovskite solar cell with the inverted architecture, the large V_{oc} loss still exists [$E_g - V_{oc}^{measured} = 0.81$ eV, see Fig. 6(b)]. The theoretical V_{oc} limit for $FA_{0.75}MA_{0.25}SnI_3$ is $V_{oc}^{limit} = 1.08$ eV, considering its E_g of 1.36 eV and detailed balance theory.[163] Even in the tin-based solar cells with a record efficiency (9.6%), the voltage loss is large: $E_g - V_{oc}^{measured} = 0.88$ eV.[38] For comparison, the reported V_{oc} loss in the high-efficiency $MAPbI_3$ cells is extremely small, $E_g - V_{oc}^{measured} = 0.35$ eV, which approaches the detailed balance limit.[164] Also, in the Pb–Sn mixed-type perovskites, relatively small V_{oc} losses have been reported.[58] One of the losses responsible for the drop from the detailed balance limit V_{oc}^{limit} is the loss through nonradiative recombination.[53–55,165] In the tin perovskite thin films, the PL quantum efficiency is only about 3%–10%,[166] and the EQE of a LED device operated under a current density similar to that of solar cell operation is 0.72%.[167] The corresponding nonradiative voltage loss can be calculated as $|kT/q \cdot \ln(\eta_{LED})| \approx 0.13$ eV for $T = 300$ K. Obviously, this is not enough to fully explain the observed V_{oc} deficit. The additional loss, $V_{oc}^{limit} - V_{oc}^{measured} - |kT/q \cdot \ln(\eta_{LED})|$, is about 0.4 eV. This large value suggests that the influence from interface recombination is large, rather than bulk-like recombination.[168–171] Other mechanisms may exist as well. For example, it has been pointed out that the valence band maximum of the tin iodide perovskites is higher than the highest occupied molecular orbital (HOMO) of the existing hole transport materials, which prevents efficient carrier extraction.[94,172,173] Energy levels for tin iodide perovskites and typical hole transport materials are compiled in Ref. 94. This data would suggest that hole transport materials with a higher HOMO level, such as PEDOT, could be beneficial for the V_{oc} improvement. A more detailed discussion on the V_{oc} losses may be achieved by using electroluminescence measurements.[174–177]

V. SUMMARY AND OUTLOOK

This Perspective summarized the intrinsic optical properties and the energy loss mechanisms in tin halide perovskites by considering the steady-state optical spectra and the photocarrier dynamics. It was shown that the steady-state optical properties of tin halide perovskites are very similar to those of lead halide perovskites,

i.e., a PL with almost no Stokes shift, an efficient electron–phonon interaction, and a sharp Urbach tail were observed. However, from the viewpoint of the recombination kinetics of photocarriers, an increase of the carrier lifetime is essential for the improvement of the conversion efficiencies of tin-based perovskite solar cells. The relation between the carrier dynamics and the device properties was discussed to provide possible solutions for the low conversion efficiencies.

While the explanations in this Perspective laid emphasis on the solar cell operation, tin halide perovskites can also be considered as materials for various other optoelectronic devices, such as lasers,[166,178] LEDs,[167,179] and transistors.[180,181] The intrinsic optical properties summarized in this work are essentially important for these optoelectronic applications.

At present, the PL quantum efficiencies of tin halide perovskites are still low due to the large number of nonradiative recombination centers. On the other hand, the steady-state PL data verified that they possess a high potential for application in optoelectronics. A better film quality through improvements in film deposition techniques or developments of other processing steps is essential for further progress. If the PL quantum efficiency and carrier lifetimes can be increased, tin halide perovskites can be considered as a powerful alternative to the lead-based perovskites.

ACKNOWLEDGMENTS

The authors thank our colleagues for their help and discussions. Part of this work was supported by JST-CREST (Grant No. JPMJCR16N3 to Y.K.), JST-ALCA (Grant No. JPMJAL1603 to A.W.), and KAKENHI (Grant No. 17J09650 to T.H.).

REFERENCES

[1] A. Poglitsch and D. Weber, J. Chem. Phys. **87**, 6373 (1987).
[2] B. Saparov and D. B. Mitzi, Chem. Rev. **116**, 4558 (2016).
[3] T. Ishihara, *Optical Properties of Low-Dimensional Materials*, edited by T. Ogawa and Y. Kanemitsu (World Scientific, Singapore, 1995), pp. 288–339.
[4] M. Era, S. Morimoto, T. Tsutsui, and S. Saito, Appl. Phys. Lett. **65**, 676 (1994).
[5] T. Kondo, T. Azuma, T. Yuasa, and R. Ito, Solid State Commun. **105**, 253 (1998).
[6] A. Kojima, K. Teshima, Y. Shirai, and T. Miyasaka, J. Am. Chem. Soc. **131**, 6050 (2009).
[7] M. M. Lee, J. Teuscher, T. Miyasaka, T. N. Murakami, and H. J. Snaith, Science **338**, 643 (2012).
[8] H.-S. Kim, C.-R. Lee, J.-H. Im, K.-B. Lee, T. Moehl, A. Marchioro, S.-J. Moon, R. Humphry-Baker, J.-H. Yum, J. E. Moser, M. Grätzel, and N.-G. Park, Sci. Rep. **2**, 591 (2012).
[9] Y. Kanemitsu, J. Mater. Chem. C **5**, 3427 (2017).
[10] Y. Kanemitsu and T. Handa, Jpn. J. Appl. Phys. **57**, 090101 (2018).
[11] Y. Yamada, T. Nakamura, M. Endo, A. Wakamiya, and Y. Kanemitsu, J. Am. Chem. Soc. **136**, 11610 (2014).
[12] S. D. Stranks, V. M. Burlakov, T. Leijtens, J. M. Ball, A. Goriely, and H. J. Snaith, Phys. Rev. Appl. **2**, 034007 (2014).
[13] F. Deschler, M. Price, S. Pathak, L. E. Klintberg, D. D. Jarausch, R. Higler, S. Hüttner, T. Leijtens, S. D. Stranks, H. J. Snaith, M. Atatüre, R. T. Phillips, and R. H. Friend, J. Phys. Chem. Lett. **5**, 1421 (2014).
[14] C. M. Sutter-Fella, Y. Li, M. Amani, J. W. Ager III, F. M. Toma, E. Yablonovitch, I. D. Sharp, and A. Javey, Nano Lett. **16**, 800 (2016).
[15] T. Yamada, Y. Yamada, Y. Nakaike, A. Wakamiya, and Y. Kanemitsu, Phys. Rev. Appl. **7**, 014001 (2017).
[16] I. L. Braly, D. W. deQuilettes, L. M. Pazos-Outón, S. Burke, M. E. Ziffer, D. S. Ginger, and H. W. Hillhouse, Nat. Photonics **12**, 355 (2018).
[17] Y. Yamada, T. Yamada, L. Q. Phuong, N. Maruyama, H. Nishimura, A. Wakamiya, Y. Murata, and Y. Kanemitsu, J. Am. Chem. Soc. **137**, 10456 (2015).
[18] T. Yamada, Y. Yamada, H. Nishimura, Y. Nakaike, A. Wakamiya, Y. Murata, and Y. Kanemitsu, Adv. Electron. Mater. **2**, 1500290 (2016).
[19] L. M. Pazos-Outón, M. Szumilo, R. Lamboll, J. M. Richter, M. Crespo-Quesada, M. Abdi-Jalebi, H. J. Beeson, M. Vrućinić, M. Alsari, H. J. Snaith, B. Ehrler, R. H. Friend, and F. Deschler, Science **351**, 1430 (2016).
[20] Y. Fang, H. Wei, Q. Dong, and J. Huang, Nat. Commun. **8**, 14417 (2017).
[21] T. Yamada, T. Aharen, and Y. Kanemitsu, Phys. Rev. Lett. **120**, 057404 (2018).
[22] Z.-K. Tan, R. S. Moghaddam, M. L. Lai, P. Docampo, R. Higler, F. Deschler, M. Price, A. Sadhanala, L. M. Pazos, D. Credgington, F. Hanusch, T. Bein, H. J. Snaith, and R. H. Friend, Nat. Nanotechnol. **9**, 687 (2014).
[23] K. Lin, J. Xing, L. N. Quan, F. P. G. de Arquer, X. Gong, J. Lu, L. Xie, W. Zhao, D. Zhang, C. Yan, W. Li, X. Liu, Y. Lu, J. Kirman, E. H. Sargent, Q. Xiong, and Z. Wei, Nature **562**, 245 (2018).
[24] Y. Cao, N. Wang, H. Tian, J. Guo, Y. Wei, H. Chen, Y. Miao, W. Zou, K. Pan, Y. He, H. Cao, Y. Ke, M. Xu, Y. Wang, M. Yang, K. Du, Z. Fu, D. Kong, D. Dai, Y. Jin, G. Li, H. Li, Q. Peng, J. Wang, and W. Huang, Nature **562**, 249 (2018).
[25] S.-T. Ha, C. Shen, J. Zhang, and Q. Xiong, Nat. Photonics **10**, 115 (2016).
[26] T. Yamada, T. Aharen, and Y. Kanemitsu, Phys. Rev. Mater. **3**, 024601 (2019).
[27] H. Hirori, P. Xia, Y. Shinohara, T. Otobe, Y. Sanari, H. Tahara, N. Ishii, J. Itatani, K. L. Ishikawa, T. Aharen, M. Ozaki, A. Wakamiya, and Y. Kanemitsu, APL Mater. **7**, 041107 (2019).
[28] H. Tahara, T. Aharen, A. Wakamiya, and Y. Kanemitsu, Adv. Opt. Mater. **6**, 1701366 (2018).
[29] F. Hao, C. C. Stoumpos, D. H. Cao, R. P. H. Chang, and M. G. Kanatzidis, Nat. Photonics **8**, 489 (2014).
[30] N. K. Noel, S. D. Stranks, A. Abate, C. Wehrenfennig, S. Guarnera, A.-A. Haghighirad, A. Sadhanala, G. E. Eperon, S. K. Pathak, M. B. Johnston, A. Petrozza, L. M. Herz, and H. J. Snaith, Energy Environ. Sci. **7**, 3061 (2014).
[31] M. H. Kumar, S. Dharani, W. L. Leong, P. P. Boix, R. R. Prabhakar, T. Baikie, C. Shi, H. Ding, R. Ramesh, M. Asta, M. Graetzel, S. G. Mhaisalkar, and N. Mathews, Adv. Mater. **26**, 7122 (2014).
[32] T. M. Koh, T. Krishnamoorthy, N. Yantara, C. Shi, W. L. Leong, P. P. Boix, A. C. Grimsdale, S. G. Mhaisalkar, and N. Mathews, J. Mater. Chem. A **3**, 14996 (2015).
[33] A. H. Slavney, T. Hu, A. M. Lindenberg, and H. I. Karunadasa, J. Am. Chem. Soc. **138**, 2138 (2016).
[34] R. L. Z. Hoye, R. E. Brandt, A. Osherov, V. Stevanović, S. D. Stranks, M. W. B. Wilson, H. Kim, A. J. Akey, J. D. Perkins, R. C. Kurchin, J. R. Poindexter, E. N. Wang, M. G. Bawendi, V. Bulović, and T. Buonassisi, Chem. - A Eur. J. **22**, 2605 (2016).
[35] A. Koedtruad, M. Goto, M. Amano Patino, Z. Tan, H. Guo, T. Nakamura, T. Handa, W.-T. Chen, Y.-C. Chuang, H.-S. Sheu, T. Saito, D. Kan, Y. Kanemitsu, A. Wakamiya, and Y. Shimakawa, J. Mater. Chem. A **7**, 5583 (2019).
[36] T. Krishnamoorthy, H. Ding, C. Yan, W. L. Leong, T. Baikie, Z. Zhang, M. Sherburne, S. Li, M. Asta, N. Mathews, and S. G. Mhaisalkar, J. Mater. Chem. A **3**, 23829 (2015).
[37] T. Jun, K. Sim, S. Iimura, M. Sasase, H. Kamioka, J. Kim, and H. Hosono, Adv. Mater. **30**, 1804547 (2018).
[38] E. Jokar, C.-H. Chien, C.-M. Tsai, A. Fathi, and E. W.-G. Diau, Adv. Mater. **31**, 1804835 (2019).
[39] See https://www.nrel.gov/pv/cell-efficiency.html for National Renewable Energy Laboratory Research Cell Efficiency Records; accessed 4 May 2019.
[40] M. A. Green, Y. Hishikawa, E. D. Dunlop, D. H. Levi, J. Hohl-Ebinger, M. Yoshita, and A. W. Y. Ho-Baillie, Prog. Photovoltaics Res. Appl. **27**, 3 (2019).
[41] E. H. Jung, N. J. Jeon, E. Y. Park, C. S. Moon, T. J. Shin, T.-Y. Yang, J. H. Noh, and J. Seo, Nature **567**, 511 (2019).
[42] Q. Jiang, Y. Zhao, X. Zhang, X. Yang, Y. Chen, Z. Chu, Q. Ye, X. Li, Z. Yin, and J. You, Nat. Photonics **13**, 460 (2019).
[43] V. M. Goldschmidt, Ber. Dtsch. Chem. Ges., Ser. A, B **60**, 1263 (1927).

[44]C. Li, X. Lu, W. Ding, L. Feng, Y. Gao, and Z. Guo, Acta Crystallogr. Sect., B Struct. Sci. **64**, 702 (2008).
[45]C. J. Bartel, C. Sutton, B. R. Goldsmith, R. Ouyang, C. B. Musgrave, L. M. Ghiringhelli, and M. Scheffler, Sci. Adv. **5**, eaav0693 (2019).
[46]J. H. Noh, S. H. Im, J. H. Heo, T. N. Mandal, and S. Il Seok, Nano Lett. **13**, 1764 (2013).
[47]M. Saliba, T. Matsui, J.-Y. Seo, K. Domanski, J.-P. Correa-Baena, M. K. Nazeeruddin, S. M. Zakeeruddin, W. Tress, A. Abate, A. Hagfeldt, and M. Grätzel, Energy Environ. Sci. **9**, 1989 (2016).
[48]M. Saliba, T. Matsui, K. Domanski, J.-Y. Seo, A. Ummadisingu, S. M. Zakeeruddin, J.-P. Correa-Baena, W. R. Tress, A. Abate, A. Hagfeldt, and M. Grätzel, Science **354**, 206 (2016).
[49]G. Xing, N. Mathews, S. S. Lim, N. Yantara, X. Liu, D. Sabba, M. Grätzel, S. Mhaisalkar, and T. C. Sum, Nat. Mater. **13**, 476 (2014).
[50]H. Zhu, Y. Fu, F. Meng, X. Wu, Z. Gong, Q. Ding, M. V. Gustafsson, M. T. Trinh, S. Jin, and X.-Y. Zhu, Nat. Mater. **14**, 636 (2015).
[51]S. Shao, Y. Cui, H. Duim, X. Qiu, J. Dong, G. H. ten Brink, G. Portale, R. C. Chiechi, S. Zhang, J. Hou, and M. A. Loi, Adv. Mater. **30**, 1803703 (2018).
[52]L. Q. Phuong, I. L. Braly, J. K. Katahara, H. W. Hillhouse, and Y. Kanemitsu, Appl. Phys. Express **10**, 102401 (2017).
[53]W. Shockley and H. J. Queisser, J. Appl. Phys. **32**, 510 (1961).
[54]L. Zhu, T. Mochizuki, M. Yoshita, S. Chen, C. Kim, H. Akiyama, and Y. Kanemitsu, Opt. Express **24**, A740 (2016).
[55]O. D. Miller, E. Yablonovitch, and S. R. Kurtz, IEEE J. Photovoltaics **2**, 303 (2012).
[56]G. E. Eperon, S. D. Stranks, C. Menelaou, M. B. Johnston, L. M. Herz, and H. J. Snaith, Energy Environ. Sci. **7**, 982 (2014).
[57]F. Hao, C. C. Stoumpos, R. P. H. Chang, and M. G. Kanatzidis, J. Am. Chem. Soc. **136**, 8094 (2014).
[58]B. Zhao, M. Abdi-Jalebi, M. Tabachnyk, H. Glass, V. S. Kamboj, W. Nie, A. J. Pearson, Y. Puttisong, K. C. Gödel, H. E. Beere, D. A. Ritchie, A. D. Mohite, S. E. Dutton, R. H. Friend, and A. Sadhanala, Adv. Mater. **29**, 1604744 (2017).
[59]G. E. Eperon, T. Leijtens, K. A. Bush, R. Prasanna, T. Green, J. T.-W. Wang, D. P. McMeekin, G. Volonakis, R. L. Milot, R. May, A. Palmstrom, D. J. Slotcavage, R. A. Belisle, J. B. Patel, E. S. Parrott, R. J. Sutton, W. Ma, F. Moghadam, B. Conings, A. Babayigit, H.-G. Boyen, S. Bent, F. Giustino, L. M. Herz, M. B. Johnston, M. D. McGehee, and H. J. Snaith, Science **354**, 861 (2016).
[60]R. Prasanna, A. Gold-Parker, T. Leijtens, B. Conings, A. Babayigit, H. G. Boyen, M. F. Toney, and M. D. McGehee, J. Am. Chem. Soc. **139**, 11117 (2017).
[61]J. Im, C. C. Stoumpos, H. Jin, A. J. Freeman, and M. G. Kanatzidis, J. Phys. Chem. Lett. **6**, 3503 (2015).
[62]A. Goyal, S. McKechnie, D. Pashov, W. Tumas, M. van Schilfgaarde, and V. Stevanović, Chem. Mater. **30**, 3920 (2018).
[63]Y. Tian and I. G. Scheblykin, J. Phys. Chem. Lett. **6**, 3466 (2015).
[64]T. Handa, T. Yamada, H. Kubota, S. Ise, Y. Miyamoto, and Y. Kanemitsu, J. Phys. Chem. C **121**, 16158 (2017).
[65]Y. Yamada, T. Nakamura, M. Endo, A. Wakamiya, and Y. Kanemitsu, Appl. Phys. Express **7**, 032302 (2014).
[66]P. Umari, E. Mosconi, and F. De Angelis, Sci. Rep. **4**, 4467 (2014).
[67]A. M. A. Leguy, P. Azarhoosh, M. I. Alonso, M. Campoy-Quiles, O. J. Weber, J. Yao, D. Bryant, M. T. Weller, J. Nelson, A. Walsh, M. van Schilfgaarde, and P. R. F. Barnes, Nanoscale **8**, 6317 (2016).
[68]M. Shirayama, H. Kadowaki, T. Miyadera, T. Sugita, M. Tamakoshi, M. Kato, T. Fujiseki, D. Murata, S. Hara, T. N. Murakami, S. Fujimoto, M. Chikamatsu, and H. Fujiwara, Phys. Rev. Appl. **5**, 014012 (2016).
[69]S. De Wolf, J. Holovsky, S.-J. Moon, P. Löper, B. Niesen, M. Ledinsky, F.-J. Haug, J.-H. Yum, and C. Ballif, J. Phys. Chem. Lett. **5**, 1035 (2014).
[70]M. Ledinsky, T. Schönfeldová, J. Holovský, E. Aydin, Z. Hájková, L. Landová, N. Neyková, A. Fejfar, and S. De Wolf, J. Phys. Chem. Lett. **10**, 1368 (2019).
[71]Y. Yamada, T. Nakamura, M. Endo, A. Wakamiya, and Y. Kanemitsu, IEEE J. Photovoltaics **5**, 401 (2015).
[72]Y. Yamada, M. Endo, A. Wakamiya, and Y. Kanemitsu, J. Phys. Chem. Lett. **6**, 482 (2015).
[73]L. Q. Phuong, Y. Nakaike, A. Wakamiya, and Y. Kanemitsu, J. Phys. Chem. Lett. **7**, 4905 (2016).
[74]A. D. Wright, C. Verdi, R. L. Milot, G. E. Eperon, M. A. Pérez-Osorio, H. J. Snaith, F. Giustino, M. B. Johnston, and L. M. Herz, Nat. Commun. **7**, 11755 (2016).
[75]J. Tilchin, D. N. Dirin, G. I. Maikov, A. Sashchiuk, M. V. Kovalenko, and E. Lifshitz, ACS Nano **10**, 6363 (2016).
[76]M. Nagai, T. Tomioka, M. Ashida, M. Hoyano, R. Akashi, Y. Yamada, T. Aharen, and Y. Kanemitsu, Phys. Rev. Lett. **121**, 145506 (2018).
[77]C. Wehrenfennig, M. Liu, H. J. Snaith, M. B. Johnston, and L. M. Herz, J. Phys. Chem. Lett. **5**, 1300 (2014).
[78]Y. Kanemitsu, M. Okano, L. Q. Phuong, and Y. Yamada, ECS J. Solid State Sci. Technol. **7**, R3102 (2018).
[79]Y. Yamada, T. Yamada, and Y. Kanemitsu, Bull. Chem. Soc. Jpn. **90**, 1129 (2017).
[80]A. Miyata, A. Mitioglu, P. Plochocka, O. Portugall, J. T.-W. Wang, S. D. Stranks, H. J. Snaith, and R. J. Nicholas, Nat. Phys. **11**, 582 (2015).
[81]K. Galkowski, A. Mitioglu, A. Miyata, P. Plochocka, O. Portugall, G. E. Eperon, J. T.-W. Wang, T. Stergiopoulos, S. D. Stranks, H. J. Snaith, and R. J. Nicholas, Energy Environ. Sci. **9**, 962 (2016).
[82]S. D. Stranks, G. E. Eperon, G. Grancini, C. Menelaou, M. J. P. Alcocer, T. Leijtens, L. M. Herz, A. Petrozza, and H. J. Snaith, Science **342**, 341 (2013).
[83]Q. Dong, Y. Fang, Y. Shao, P. Mulligan, J. Qiu, L. Cao, and J. Huang, Science **347**, 967 (2015).
[84]D. Webber, C. Clegg, A. W. Mason, S. A. March, I. G. Hill, and K. C. Hall, Appl. Phys. Lett. **111**, 121905 (2017).
[85]E. S. Parrott, R. L. Milot, T. Stergiopoulos, H. J. Snaith, M. B. Johnston, and L. M. Herz, J. Phys. Chem. Lett. **7**, 1321 (2016).
[86]T. R. Arend, M. Tönnies, P. Reisbeck, C. J. P. Rieckmann, and R. Kersting, Phys. Status Solidi Appl. Mater. Sci. **214**, 1600796 (2017).
[87]F. Hao, C. C. Stoumpos, P. Guo, N. Zhou, T. J. Marks, R. P. H. Chang, and M. G. Kanatzidis, J. Am. Chem. Soc. **137**, 11445 (2015).
[88]T. Yokoyama, D. H. Cao, C. C. Stoumpos, T.-B. Song, Y. Sato, S. Aramaki, and M. G. Kanatzidis, J. Phys. Chem. Lett. **7**, 776 (2016).
[89]M. Konstantakou and T. Stergiopoulos, J. Mater. Chem. A **5**, 11518 (2017).
[90]Z. Zhu, C.-C. Chueh, N. Li, C. Mao, and A. K. Y. Jen, Adv. Mater. **30**, 1703800 (2018).
[91]N. J. Jeon, J. H. Noh, Y. C. Kim, W. S. Yang, S. Ryu, and S. Il Seok, Nat. Mater. **13**, 897 (2014).
[92]W. Liao, D. Zhao, Y. Yu, C. R. Grice, C. Wang, A. J. Cimaroli, P. Schulz, W. Meng, K. Zhu, R. G. Xiong, and Y. Yan, Adv. Mater. **28**, 9333 (2016).
[93]T. Fujihara, S. Terakawa, T. Matsushima, C. Qin, M. Yahiro, and C. Adachi, J. Mater. Chem. C **5**, 1121 (2017).
[94]M. Ozaki, Y. Katsuki, J. Liu, T. Handa, R. Nishikubo, S. Yakumaru, Y. Hashikawa, Y. Murata, T. Saito, Y. Shimakawa, Y. Kanemitsu, A. Saeki, and A. Wakamiya, ACS Omega **2**, 7016 (2017).
[95]J. Liu, M. Ozaki, S. Yakumaru, T. Handa, R. Nishikubo, Y. Kanemitsu, A. Saeki, Y. Murata, R. Murdey, and A. Wakamiya, Angew. Chem., Int. Ed. **57**, 13221 (2018).
[96]L. Zhu, H. Akiyama, and Y. Kanemitsu, Sci. Rep. **8**, 11704 (2018).
[97]Y. Takahashi, R. Obara, Z.-Z. Lin, Y. Takahashi, T. Naito, T. Inabe, S. Ishibashi, and K. Terakura, Dalt. Trans. **40**, 5563 (2011).
[98]Y. Takahashi, H. Hasegawa, Y. Takahashi, and T. Inabe, J. Solid State Chem. **205**, 39 (2013).
[99]S. J. Lee, S. S. Shin, Y. C. Kim, D. Kim, T. K. Ahn, J. H. Noh, J. Seo, and S. Il Seok, J. Am. Chem. Soc. **138**, 3974 (2016).
[100]R. L. Milot, M. T. Klug, C. L. Davies, Z. Wang, H. Kraus, H. J. Snaith, M. B. Johnston, and L. M. Herz, Adv. Mater. **30**, 1804506 (2018).
[101]S. Gupta, D. Cahen, and G. Hodes, J. Phys. Chem. C **122**, 13926 (2018).
[102]E. Burstein, Phys. Rev. **93**, 632 (1954).
[103]T. S. Moss, Proc. Phys. Soc. Sect. B **67**, 775 (1954).
[104]J. I. Pankove, Phys. Rev. **140**, A2059 (1965).
[105]D. Olego and M. Cardona, Phys. Rev. B **22**, 886 (1980).

[106]H.-C. Wang, W. Wang, A.-C. Tang, H.-Y. Tsai, Z. Bao, T. Ihara, N. Yarita, H. Tahara, Y. Kanemitsu, S. Chen, and R.-S. Liu, Angew. Chem., Int. Ed. **56**, 13650 (2017).
[107]N. Yarita, H. Tahara, T. Ihara, T. Kawawaki, R. Sato, M. Saruyama, T. Teranishi, and Y. Kanemitsu, J. Phys. Chem. Lett. **8**, 1413 (2017).
[108]B. A. Koscher, J. K. Swabeck, N. D. Bronstein, and A. P. Alivisatos, J. Am. Chem. Soc. **139**, 6566 (2017).
[109]N. Yarita, H. Tahara, M. Saruyama, T. Kawawaki, R. Sato, T. Teranishi, and Y. Kanemitsu, J. Phys. Chem. Lett. **8**, 6041 (2017).
[110]S. Nakahara, H. Tahara, G. Yumoto, T. Kawawaki, M. Saruyama, R. Sato, T. Teranishi, and Y. Kanemitsu, J. Phys. Chem. C **122**, 22188 (2018).
[111]N. Yarita, T. Aharen, H. Tahara, M. Saruyama, T. Kawawaki, R. Sato, T. Teranishi, and Y. Kanemitsu, Phys. Rev. Mater. **2**, 116003 (2018).
[112]D. P. Nenon, K. Pressler, J. Kang, B. A. Koscher, J. H. Olshansky, W. T. Osowiecki, M. A. Koc, L.-W. Wang, and A. P. Alivisatos, J. Am. Chem. Soc. **140**, 17760 (2018).
[113]C. C. Stoumpos, C. D. Malliakas, and M. G. Kanatzidis, Inorg. Chem. **52**, 9019 (2013).
[114]Y. Yamada, M. Hoyano, R. Akashi, K. Oto, and Y. Kanemitsu, J. Phys. Chem. Lett. **8**, 5798 (2017).
[115]R. E. Brandt, V. Stevanović, D. S. Ginley, and T. Buonassisi, MRS Commun. **5**, 265 (2015).
[116]P. Y. Yu and M. Cardona, *Fundamentals of Semiconductors*, 4th ed. (Springer Berlin Heidelberg, Berlin, Heidelberg, 2010).
[117]X. Y. Zhu and V. Podzorov, J. Phys. Chem. Lett. **6**, 4758 (2015).
[118]M. B. Price, J. Butkus, T. C. Jellicoe, A. Sadhanala, A. Briane, J. E. Halpert, K. Broch, J. M. Hodgkiss, R. H. Friend, and F. Deschler, Nat. Commun. **6**, 8420 (2015).
[119]Y. Yang, D. P. Ostrowski, R. M. France, K. Zhu, J. van de Lagemaat, J. M. Luther, and M. C. Beard, Nat. Photonics **10**, 53 (2016).
[120]H. Zhu, K. Miyata, Y. Fu, J. Wang, P. P. Joshi, D. Niesner, K. W. Williams, S. Jin, and X.-Y. Zhu, Science **353**, 1409 (2016).
[121]D. Niesner, H. Zhu, K. Miyata, P. P. Joshi, T. J. S. Evans, B. J. Kudisch, M. T. Trinh, M. Marks, and X. Y. Zhu, J. Am. Chem. Soc. **138**, 15717 (2016).
[122]A. Y. Chang, Y.-J. Cho, K.-C. Chen, C.-W. Chen, A. Kinaci, B. T. Diroll, M. J. Wagner, M. K. Y. Chan, H.-W. Lin, and R. D. Schaller, Adv. Energy Mater. **6**, 1600422 (2016).
[123]M. Sendner, P. K. Nayak, D. A. Egger, S. Beck, C. Müller, B. Epding, W. Kowalsky, L. Kronik, H. J. Snaith, A. Pucci, and R. Lovrinčić, Mater. Horizons **3**, 613 (2016).
[124]J. M. Frost, L. D. Whalley, and A. Walsh, ACS Energy Lett. **2**, 2647 (2017).
[125]H. Zhu, M. T. Trinh, J. Wang, Y. Fu, P. P. Joshi, K. Miyata, S. Jin, and X.-Y. Zhu, Adv. Mater. **29**, 1603072 (2017).
[126]O. Yaffe, Y. Guo, L. Z. Tan, D. A. Egger, T. Hull, C. C. Stoumpos, F. Zheng, T. F. Heinz, L. Kronik, M. G. Kanatzidis, J. S. Owen, A. M. Rappe, M. A. Pimenta, and L. E. Brus, Phys. Rev. Lett. **118**, 136001 (2017).
[127]M. Li, S. Bhaumik, T. W. Goh, M. S. Kumar, N. Yantara, M. Grätzel, S. Mhaisalkar, N. Mathews, and T. C. Sum, Nat. Commun. **8**, 14350 (2017).
[128]J. Fu, Q. Xu, G. Han, B. Wu, C. H. A. Huan, M. L. Leek, and T. C. Sum, Nat. Commun. **8**, 1300 (2017).
[129]T. Ghosh, S. Aharon, L. Etgar, and S. Ruhman, J. Am. Chem. Soc. **139**, 18262 (2017).
[130]K. Miyata, D. Meggiolaro, M. T. Trinh, P. P. Joshi, E. Mosconi, S. C. Jones, F. De Angelis, and X.-Y. Zhu, Sci. Adv. **3**, e1701217 (2017).
[131]J. Yang, X. Wen, H. Xia, R. Sheng, Q. Ma, J. Kim, P. Tapping, T. Harada, T. W. Kee, F. Huang, Y.-B. Cheng, M. Green, A. Ho-Baillie, S. Huang, S. Shrestha, R. Patterson, and G. Conibeer, Nat. Commun. **8**, 14120 (2017).
[132]G. Batignani, G. Fumero, A. R. Srimath Kandada, G. Cerullo, M. Gandini, C. Ferrante, A. Petrozza, and T. Scopigno, Nat. Commun. **9**, 1971 (2018).
[133]T. R. Hopper, A. Gorodetsky, J. M. Frost, C. Müller, R. Lovrincic, and A. A. Bakulin, ACS Energy Lett. **3**, 2199 (2018).
[134]T. Handa, T. Aharen, A. Wakamiya, and Y. Kanemitsu, Phys. Rev. Mater. **2**, 075402 (2018).
[135]K. Wu, A. Bera, C. Ma, Y. Du, Y. Yang, L. Li, and T. Wu, Phys. Chem. Chem. Phys. **16**, 22476 (2014).
[136]L. Q. Phuong, Y. Yamada, M. Nagai, N. Maruyama, A. Wakamiya, and Y. Kanemitsu, J. Phys. Chem. Lett. **7**, 2316 (2016).
[137]K. Appavoo, W. Nie, J.-C. Blancon, J. Even, A. D. Mohite, and M. Y. Sfeir, Phys. Rev. B **96**, 195308 (2017).
[138]Z. M. Gibbs, H. Kim, H. Wang, R. L. White, F. Drymiotis, M. Kaviany, and G. J. Snyder, Appl. Phys. Lett. **103**, 262109 (2013).
[139]A. Göbel, T. Ruf, M. Cardona, C. T. Lin, J. Wrzesinski, M. Steube, K. Reimann, J.-C. Merle, and M. Joucla, Phys. Rev. B **57**, 15183 (1998).
[140]M. I. Dar, G. Jacopin, S. Meloni, A. Mattoni, N. Arora, A. Boziki, S. M. Zakeeruddin, U. Rothlisberger, and M. Grätzel, Sci. Adv. **2**, e1601156 (2016).
[141]J. Lee, E. S. Koteles, and M. O. Vassell, Phys. Rev. B **33**, 5512 (1986).
[142]E. Daub and P. Würfel, Phys. Rev. Lett. **74**, 1020 (1995).
[143]C. Barugkin, J. Cong, T. Duong, S. Rahman, H. T. Nguyen, D. Macdonald, T. P. White, and K. R. Catchpole, J. Phys. Chem. Lett. **6**, 767 (2015).
[144]I. Chung, J. H. Song, J. Im, J. Androulakis, C. D. Malliakas, H. Li, A. J. Freeman, J. T. Kenney, and M. G. Kanatzidis, J. Am. Chem. Soc. **134**, 8579 (2012).
[145]H. Oga, A. Saeki, Y. Ogomi, S. Hayase, and S. Seki, J. Am. Chem. Soc. **136**, 13818 (2014).
[146]C. Wehrenfennig, G. E. Eperon, M. B. Johnston, H. J. Snaith, and L. M. Herz, Adv. Mater. **26**, 1584 (2014).
[147]R. L. Milot, G. E. Eperon, H. J. Snaith, M. B. Johnston, and L. M. Herz, Adv. Funct. Mater. **25**, 6218 (2015).
[148]O. G. Reid, M. Yang, N. Kopidakis, K. Zhu, and G. Rumbles, ACS Energy Lett. **1**, 561 (2016).
[149]K. Galkowski, A. Surrente, M. Baranowski, B. Zhao, Z. Yang, A. Sadhanala, S. Mackowski, S. D. Stranks, and P. Plochocka, ACS Energy Lett. **4**, 615 (2019).
[150]C.-H. M. Chuang, A. Maurano, R. E. Brandt, G. W. Hwang, J. Jean, T. Buonassisi, V. Bulović, and M. G. Bawendi, Nano Lett. **15**, 3286 (2015).
[151]N. Ahn, D. Y. Son, I. H. Jang, S. M. Kang, M. Choi, and N. G. Park, J. Am. Chem. Soc. **137**, 8696 (2015).
[152]A. Polman, M. Knight, E. C. Garnett, B. Ehrler, and W. C. Sinke, Science **352**, aad4424 (2016).
[153]S. Shao, J. Liu, G. Portale, H.-H. Fang, G. R. Blake, G. H. ten Brink, L. J. A. Koster, and M. A. Loi, Adv. Energy Mater. **8**, 1702019 (2018).
[154]W. Ke, C. C. Stoumpos, and M. G. Kanatzidis, "Unleaded' perovskites: Status quo and future prospects of tin-based perovskite solar cells," Adv. Mater. (published online 2018).
[155]Z. Zhao, F. Gu, Y. Li, W. Sun, S. Ye, H. Rao, Z. Liu, Z. Bian, and C. Huang, Adv. Sci. **4**, 1700204 (2017).
[156]D. M. Tex, T. Ihara, H. Akiyama, M. Imaizumi, and Y. Kanemitsu, Appl. Phys. Lett. **106**, 013905 (2015).
[157]D. M. Tex, M. Imaizumi, and Y. Kanemitsu, Opt. Express **23**, A1687 (2015).
[158]D. Yamashita, T. Handa, T. Ihara, H. Tahara, A. Shimazaki, A. Wakamiya, and Y. Kanemitsu, J. Phys. Chem. Lett. **7**, 3186 (2016).
[159]T. Handa, D. M. Tex, A. Shimazaki, A. Wakamiya, and Y. Kanemitsu, J. Phys. Chem. Lett. **8**, 954 (2017).
[160]D. M. Tex, M. Imaizumi, and Y. Kanemitsu, Phys. Rev. Appl. **7**, 014019 (2017).
[161]L. Ma, F. Hao, C. C. Stoumpos, B. T. Phelan, M. R. Wasielewski, and M. G. Kanatzidis, J. Am. Chem. Soc. **138**, 14750 (2016).
[162]E. M. Hutter, J.-J. Hofman, M. L. Petrus, M. Moes, R. D. Abellón, P. Docampo, and T. J. Savenije, Adv. Energy Mater. **7**, 1602349 (2017).
[163]S. Rühle, Sol. Energy **130**, 139 (2016).
[164]Z. Liu, L. Krückemeier, B. Krogmeier, B. Klingebiel, J. A. Márquez, S. Levcenko, S. Öz, S. Mathur, U. Rau, T. Unold, and T. Kirchartz, ACS Energy Lett. **4**, 110 (2019).
[165]U. Rau, Phys. Rev. B **76**, 085303 (2007).
[166]G. Xing, M. H. Kumar, W. K. Chong, X. Liu, Y. Cai, H. Ding, M. Asta, M. Grätzel, S. Mhaisalkar, N. Mathews, and T. C. Sum, Adv. Mater. **28**, 8191 (2016).
[167]M. L. Lai, T. Y. S. Tay, A. Sadhanala, S. E. Dutton, G. Li, R. H. Friend, and Z. K. Tan, J. Phys. Chem. Lett. **7**, 2653 (2016).

[168]Y. Yamada, T. Yamada, A. Shimazaki, A. Wakamiya, and Y. Kanemitsu, J. Phys. Chem. Lett. **7**, 1972 (2016).
[169]H. Do Kim, Y. Miyamoto, H. Kubota, T. Yamanari, and H. Ohkita, Chem. Lett. **46**, 253 (2017).
[170]X. Hu, X.-F. Jiang, X. Xing, L. Nian, X. Liu, R. Huang, K. Wang, H.-L. Yip, and G. Zhou, Sol. RRL **2**, 1800083 (2018).
[171]A. Zohar, M. Kulbak, I. Levine, G. Hodes, A. Kahn, and D. Cahen, ACS Energy Lett. **4**, 1 (2019).
[172]T.-B. Song, T. Yokoyama, S. Aramaki, and M. G. Kanatzidis, ACS Energy Lett. **2**, 897 (2017).
[173]R. Nishikubo, N. Ishida, Y. Katsuki, A. Wakamiya, and A. Saeki, J. Phys. Chem. C **121**, 19650 (2017).
[174]K. Tvingstedt, O. Malinkiewicz, A. Baumann, C. Deibel, H. J. Snaith, V. Dyakonov, and H. J. Bolink, Sci. Rep. **4**, 6071 (2014).
[175]M. Okano, M. Endo, A. Wakamiya, M. Yoshita, H. Akiyama, and Y. Kanemitsu, Appl. Phys. Express **8**, 102302 (2015).
[176]T. Handa, D. M. Tex, A. Shimazaki, T. Aharen, A. Wakamiya, and Y. Kanemitsu, Opt. Express **24**, A917 (2016).
[177]W. Tress, Adv. Energy Mater. **7**, 1602358 (2017).
[178]R. L. Milot, G. E. Eperon, T. Green, H. J. Snaith, M. B. Johnston, and L. M. Herz, J. Phys. Chem. Lett. **7**, 4178 (2016).
[179]W.-L. Hong, Y.-C. Huang, C.-Y. Chang, Z.-C. Zhang, H.-R. Tsai, N.-Y. Chang, and Y.-C. Chao, Adv. Mater. **28**, 8029 (2016).
[180]T. Matsushima, S. Hwang, A. S. D. Sandanayaka, C. Qin, S. Terakawa, T. Fujihara, M. Yahiro, and C. Adachi, Adv. Mater. **28**, 10275 (2016).
[181]T. Matsushima, S. Hwang, S. Terakawa, T. Fujihara, A. S. D. Sandanayaka, C. Qin, and C. Adachi, Appl. Phys. Express **10**, 024103 (2017).